

## MODELING OF STRAIN LOCALIZATION VIA A TWO-SCALE FORMULATION.

Sebastián D'heres<sup>a</sup> and Eduardo N. Dvorkin<sup>b</sup>.

<sup>a</sup> *Instituto Tecnológico de Buenos Aires. Av. E. Madero 399 C1106ACD, Buenos Aires, Argentina.*  
*sdhers@itba.edu.ar*

<sup>b</sup> *Engineering School University of Buenos Aires Materials and Structures Laboratory*  
*Av. Las Heras 2214 C1127AAR, Buenos Aires, Argentina*  
*edvorkin@fi.uba.ar*

**Key Words:** plasticity, localization, shear band, fracture, strong discontinuity, multiple scale formulation.

**Abstract.** Strain localization phenomena usually precede the failure of different materials. A two-scale finite element formulation was developed for modeling localization processes in J2 plane elastoplastic deformation processes. The formulation is based on the use of embedded strong discontinuity modes which are triggered using a stress based criterion. The new formulation does not require a specific mesh refinement to model the localization phenomena and provides mesh independent results. The shear bands constitutive behavior is derived from the continuum properties without the introduction of any ad hoc physical law.

## 1 INTRODUCTION.

The process of mechanical failure in most cases is accompanied by a localization stage where the strains tend to concentrate in small regions of the domain. This localization behavior impacts on the subsequent failure stages. In the case of brittle materials like concrete, strain localization leads to material fracture and crack opening. In ductile materials like metals, under certain stress/strain conditions, a very narrow localized zone of intense plastic deformation –named shear band– can appear, leading to intense material degradation and failure. Thus the modeling of a solid body up to its ultimate loading in such cases requires the capability of modeling the strain localization phenomena.

The difficulty in modeling strain localization phenomena using standard finite element formulations lies in the different scales that need to be used for the description of the global deformation in the continuum and the localized deformation along zero width lines. The use of standard finite element formulations for modeling brittle fracture or shear banding imposes the width of the localized zone to be in the elements size scale; hence the results are mesh-dependent.

For modeling the fracture of brittle materials like concrete, rocks and ceramics, the fracture initiation is defined by a tensile stress larger than a threshold value and during fracture propagation. Softening is observed in the load-displacement response, but since a local constitutive relation showing strain softening was proved to be thermodynamically unacceptable, the phenomenon is modeled introducing a fracture mechanics concept: the fracture energy, which has been shown to be a material property. The different finite element methodologies that were developed for modeling the fracture process in brittle materials are: the smeared crack approach (de Borst and Nauta 1985), the discrete crack approach (Hillerborg et al. 1976), embedded discontinuous strain fields (Ortiz et al. 1987) and embedded discontinuous displacement fields (Dvorkin et al 1990 and 1991).

Regarding ductile materials, many techniques have been proposed for shear band modeling: enhanced strain field (Ortiz et al. 1987), extended finite element method (Mões et al. 1999), unfitted finite elements techniques (Mergheim et al. 2005) and embedded localization modes (D'HERS and Dvorkin 2008).

In the present work developments by Dvorkin et al. (1990, 1991) are adapted for shear band localizations as presented in D'HERS and Dvorkin (2008), and the development initially implemented for QMITC elements (Dvorkin et al. 1996) is extended to mixed elements (Bathe 1996). These embedded localization modes techniques can be classified under the category of two-scale formulations, in which a fine scale is used to model the localization phenomena (fracture in brittle materials and shear banding in ductile materials). The article is organized as follows: the triggering criteria is discussed in section 2, the localization mode is presented in section 3, and the finite element implementation is shown in section 4, some results are plotted in section 5 and at last in section 6 conclusions are stated.

## 2 SHEAR BAND INCEPTION CRITERION.

We assume a J2 material model subject to elastoplastic deformations, thus the following equations apply in a Cartesian coordinate system for infinitesimal strains and isotropic hardening, Dvorkin and Goldsmith (2005)

$$\begin{aligned}
 {}^t\sigma_{ij} &= {}^tC_{ijkl}^E ({}^t\varepsilon_{kl} - {}^t\varepsilon_{kl}^P) \\
 {}^t\varepsilon_{kl}^P &= {}^t\lambda \frac{\partial {}^t f}{\partial {}^t\sigma_{kl}} \\
 {}^t f &= \frac{3}{2} {}^t s_{ij} {}^t s_{ij} - {}^t\sigma_y^2
 \end{aligned} \tag{1}$$

Were  ${}^t\sigma_{ij}$  are the components of the Cauchy stress tensor at time (configuration)  $t$ ,  ${}^tC_{ijkl}^E$  are the components of the fourth order elastic constitutive tensor,  ${}^t\varepsilon_{kl}$  are the components of the deformation tensor,  ${}^t\varepsilon_{kl}^P$  are the components of the plastic deformation tensor,  ${}^t s_{ij}$  are the components of the deviatoric part of the Cauchy stress tensor,  ${}^t f$  is the yield function and  ${}^t\sigma_y$  is the yield stress.

For plane geometry, a shear band can be characterized by a line with normal  ${}^t\mathbf{n}$  and the direction of the displacement jump  $\llbracket {}^t\mathbf{u} \rrbracket$ , which we call  ${}^t\mathbf{m}$  and a scalar bandwidth  $d$  as proposed by [Ottosen and Ruesson \(1991\)](#) and [Larsson et al. \(1993\)](#).

It has been shown by [Rice \(1976\)](#) that the band orientation can be determined from the singularity of the acoustic stress tensor, since the vanishing of the determinant of the acoustic tensor at any point in the elastoplastic continua indicates the fulfillment of the necessary bifurcation condition. The elastoplastic constitutive tensor ([Simo and Hughes 1997](#)) is, for perfect plasticity,

$${}^t\mathbb{C}^{EP} = \left( \kappa - \frac{2}{3} G \right) {}^t\mathbb{g} \otimes {}^t\mathbb{g} + 2G \mathbb{I}^4 - 2G \frac{{}^t\mathbf{s} \otimes {}^t\mathbf{s}}{{}^t\mathbf{s} \otimes {}^t\mathbf{s}} \tag{2}$$

where  ${}^t\mathbb{g}$  is the deviatoric stress tensor,  $\kappa$  the elastic bulk modulus,  $G$  the elastic tangential modulus, and  $\mathbb{I}$  the symmetric fourth order identity tensor. We indicate the tensorial product between two tensors  $a$  and  $b$  as  $ab$ .

The acoustic tensor in a direction  ${}^t\mathbf{n}$  is defined as,

$${}^t\mathbb{Q}^{EP} = {}^t\mathbf{n} \cdot {}^t\mathbb{C}^{EP} \cdot {}^t\mathbf{n} \tag{3}$$

To investigate the stress state that produces the necessary localization condition we define a new Cartesian coordinate system  ${}^t\hat{\mathbf{x}}_i$ , with  ${}^t\hat{\mathbf{x}}_1$  in the  ${}^t\mathbf{n}$ -direction and  ${}^t\hat{\mathbf{x}}_2$  in the  ${}^t\mathbf{m}$ -direction. In this system we state the conditions for the vanishing of the determinant of the acoustic tensor and after some algebra we get,

$$\det({}^t\hat{\mathbf{Q}}_{jk}) = \frac{1}{3} G^2 \frac{(3\kappa - 2G) {}^t\hat{\mathbf{s}}_{11}^2 + (3\kappa + 4G) {}^t\hat{\mathbf{s}}_{22}^2 + (3\kappa + 4G) {}^t\hat{\mathbf{s}}_{33}^2 + (6\kappa + 8G) {}^t\hat{\mathbf{s}}_{23}^2}{{}^t\hat{\mathbf{s}} : {}^t\hat{\mathbf{s}}} = 0 \tag{4}$$

It has been shown in [D'heres and Dvorkin \(2008\)](#) that for the fulfillment of the localization condition the following must hold:  ${}^t\hat{\mathbf{s}}_{12}^2 \neq 0$  or  ${}^t\hat{\mathbf{s}}_{13}^2 \neq 0$ , and  ${}^t\hat{\mathbf{s}}_{11}^2 = {}^t\hat{\mathbf{s}}_{22}^2 = {}^t\hat{\mathbf{s}}_{33}^2 = {}^t\hat{\mathbf{s}}_{23}^2 = 0$ . Therefore, for J2 plasticity, the localization criteria based on stress components is that:

- a) Stress tensor  ${}^t\mathbb{\sigma}$  must be able to fulfill the above conditions for an orientation  ${}^t\hat{\mathbf{x}}$ .

- b) The localization condition only depends on the current stress state in J2 plasticity.
- c) The localization direction will lie in a plane orthogonal to one of the stress principal axes, since  ${}^t\hat{\mathbf{S}}_{23}^2 = {}^t\hat{\mathbf{\sigma}}_{23}^2 = 0$ .
- d) The necessary condition for localization along the directions  ${}^t\hat{\mathbf{x}}$  is:  ${}^t\hat{\sigma}_{11} + {}^t\hat{\sigma}_{22} = 2 {}^t\hat{\sigma}_{33}$
- e) The sufficient conditions for localization are condition (d) together with  ${}^t\hat{\sigma}_{12}^2 \neq 0$  or  ${}^t\hat{\sigma}_{13}^2 \neq 0$ .

If localization is not reached at plasticity onset, the stress conditions may be fulfilled later on the deformation path.

### 3 LOCALIZATION MODE

The basis of the formulation is that when within an element the localization indicator triggers the inception of a shear band, the element displacement interpolation field is enriched with a strong discontinuity, see [Dvorkin et al. \(1990, 1991\)](#), along the predicted shear band direction. If the strong discontinuity in the sliding direction is used as proposed for cohesive frictional materials, element volume is not preserved and J2 incompressibility condition is not fulfilled, see [figure 1](#).

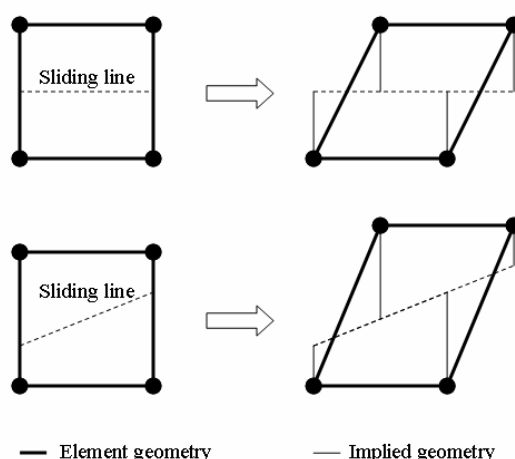


Figure 1. Volume change for sliding strong discontinuities.

Instead we introduce a displacement mode that models the local scale of the shear bands and preserves element volume to avoid such kinematic inconsistency. For this purpose we decompose the displacements into continuous scale  $\underline{\mathbf{U}}_{\text{cont}}$  and localized scale  $\underline{\mathbf{U}}_{\text{loc}}$ ,

$$\underline{\mathbf{U}} = \underline{\mathbf{U}}_{\text{cont}} + \underline{\mathbf{U}}_{\text{loc}} \quad (5)$$

Localized displacements are determined using the nodal displacements corresponding to the localized mode and a scalar value which is part of the problem unknowns.

$$\underline{\mathbf{U}}_{\text{loc}} = \gamma \underline{\Theta} \quad (6)$$

To build  $\underline{\Theta}$ , we consider that linear quadrilateral undistorted elements have 8 eigenmodes, which can be decomposed into: 3 rigid body modes, 1 volume change mode, 2 pure bending

modes and 2 pure shear modes. We use the 2 pure shear modes to build a base of pure shear modes in the isoparametric natural element space (r,s) so a pure shear eigenmode in any desired direction can be obtained as a linear combination of this "shear base". However, in the case of a distorted element, the resultant strain space has non zero volume change; hence we enhance the "shear base" with the volume change eigenmode, to enforce the plastic incompressibility. As result the vector  $\underline{\Theta}$  is determined so as to produce the maximum shear at a direction coincident with the band direction and zero volume change. The three modes, in particular for 4 node elements are shown in figure 2 and table 1, being:  ${}^t\underline{\Phi}_I$  constant tensile strain in one direction and constant compressive strain in the orthogonal direction;  ${}^t\underline{\Phi}_{II}$  constant shear strain and  ${}^t\underline{\Phi}_{III}$  constant volumetric strain. Modes extension to higher order elements is straightforward.

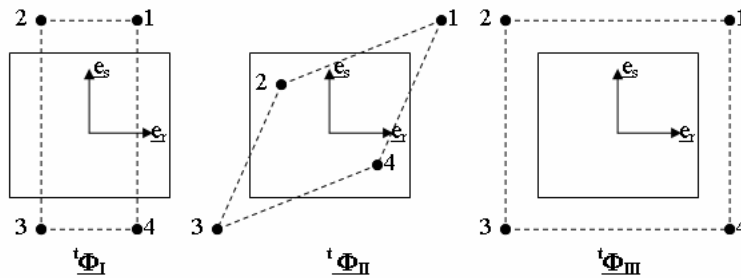


Figure 2: Deformation Modes.

	${}^t\underline{\Phi}_r^1$	${}^t\underline{\Phi}_s^1$	${}^t\underline{\Phi}_r^2$	${}^t\underline{\Phi}_s^2$	${}^t\underline{\Phi}_r^3$	${}^t\underline{\Phi}_s^3$	${}^t\underline{\Phi}_r^4$	${}^t\underline{\Phi}_s^4$
${}^t\underline{\Phi}_I$	0.5	1.5	-0.5	1.5	-0.5	-1.5	0.5	-1.5
${}^t\underline{\Phi}_{II}$	1.5	1.5	-0.5	0.5	-1.5	-1.5	0.5	-0.5
${}^t\underline{\Phi}_{III}$	1.5	1.5	-1.5	1.5	-1.5	-1.5	1.5	-1.5

Table 1: Deformation modes nodal coordinates.

The corresponding node displacements are,

$${}^t\underline{\Psi}_A^k = \left[ ({}^t\underline{\Phi}_A^k)_r - r^k \right] \underline{e}_r + \left[ ({}^t\underline{\Phi}_A^k)_s - s^k \right] \underline{e}_s \tag{7}$$

in the equation above (r,s) are the isoparametric natural coordinates,  $(\underline{e}_r, \underline{e}_s)$  are orthonormal base vectors along those directions; the subindex A=I...III indicates the deformation mode and the upper index k=1...number of nodes, indicates the node.

Displacements inside elements are interpolated in the usual manner using the shape functions  $h_k$ ,

$${}^t\underline{\Psi}_A = h_k {}^t\underline{\Psi}_A^k \tag{8}$$

The combined strains induced by the localization mode are calculated using the strain-displacements matrix calculated at the element center  $B(x_0, y_0)$  and a linear combination of

the defined displacement modes with parameters  $(\beta_I, \beta_{II}, \beta_{III})$ ,

$$\underline{\varepsilon}_{sb} = \mathbf{B}(\mathbf{x}_0, \mathbf{y}_0)(\beta_I \underline{\Psi}_I + \beta_{II} \underline{\Psi}_{II} + \beta_{III} \underline{\Psi}_{III}) \quad (9)$$

The evaluation is carried out at element center because the element volume can be exactly integrated using one point Gauss quadrature.

Stating the element incompressibility constraint in Voight notation requests,

$$\begin{aligned} (\varepsilon_1 + \varepsilon_2)_{sb} &= 0 \\ (\varepsilon_1 + \varepsilon_2 + \varepsilon_4)_{sb} &= 0 \end{aligned} \quad (10)$$

for plane stress /plane strain and axisymmetric problems respectively.

If  $\mathbf{B}(\mathbf{x}_0, \mathbf{y}_0)(\underline{\Psi}_I)$  and  $\mathbf{B}(\mathbf{x}_0, \mathbf{y}_0)(\underline{\Psi}_{II})$  are incompressible modes then  $\beta_3=0$  is adopted as no volume correction is needed; else  $\beta_3=1$ . The maximum distortion condition at an angle  $\alpha$ , defined by the shear band direction, leads to,

$$\frac{(\varepsilon_3)_{sb}}{(\varepsilon_1 - \varepsilon_2)_{sb}} = \tan\left(2\alpha + \frac{\pi}{2}\right) \quad (11)$$

Solving the Eqns. (10) and (11) the parameters  $(\beta_I, \beta_{II})$  are determined.

#### 4 VARIATIONAL FORMULATION

To determine the equilibrium equations we consider that within the continua the band has been triggered and we seek the equilibrium configuration for time  $t + \Delta t$ , via the principle of virtual work, see figure 3.

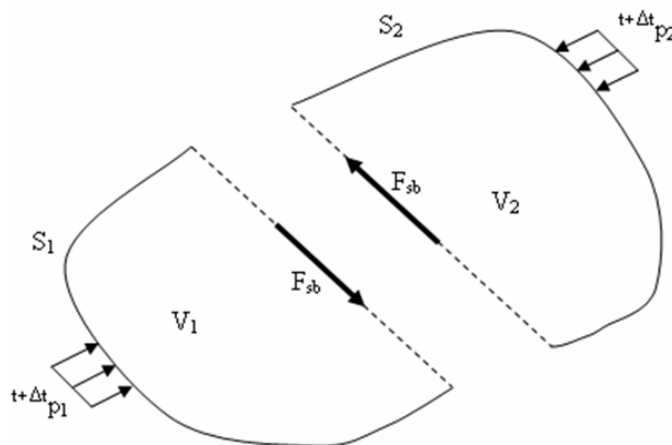


Figure 3: Localized body configuration.

We assume a geometrically linear analysis,

$$\int_{V_1+V_2} \delta(\underline{\varepsilon}_{cont})^T{}^{t+\Delta t} \underline{\sigma}_{cont} dv + \delta(\underline{U}_{sb})^T{}^{t+\Delta t} \underline{F}_{sb} = \int_{S_1} \delta \underline{u}^T{}^{t+\Delta t} \underline{p}_1 ds + \int_{S_2} \delta \underline{u}^T{}^{t+\Delta t} \underline{p}_2 ds \quad (12)$$

The vector  ${}^{t+\Delta t} \underline{F}_{sb}$  components are the nodal forces generated by the shear band localization modes. From eqns. (5) and (6) we get,

$$\begin{aligned} \underline{u}_{cont} &= \underline{H}(\underline{U} - \gamma \underline{\Theta}) \\ \underline{\varepsilon}_{cont} &= \underline{B}(\underline{U} - \gamma \underline{\Theta}) \end{aligned} \quad (13)$$

where H is the displacements interpolation matrix, B is the displacements-strains matrix, U the nodal incremental displacements and  $\gamma$  the generalized band parameter. The stress increment is evaluated at the continuum scale,

$${}^{t+\Delta t} \underline{\sigma}_{cont} = {}^t \underline{\sigma}_{cont} + {}^t \underline{C}^{EP} \underline{\varepsilon}_{cont} \quad (14)$$

To establish the band forces evolution along an incremental step we relate the continuum scale to the shear band scale postulating that the incremental localized strains equal the incremental continuum strains produced by the localized displacement mode,

$$\underline{\varepsilon}_{sb} = \underline{B} \gamma \underline{\Theta} \quad (15)$$

Hence, the relation between the incremental equivalent plastic deformation ( $\bar{\varepsilon}$ ) and the localized strains ( $\gamma$ ) is,

$$\bar{\varepsilon}^2 = \frac{2}{3} \underline{\varepsilon}_{ij}^P \underline{\varepsilon}_{ij}^P = \frac{2}{3} \underline{\varepsilon}_{sb}^T \underline{A} \underline{\varepsilon}_{sb} = \frac{2}{3} \gamma \underline{\Theta}^T \underline{B}^T \underline{A} \underline{B} \underline{\Theta} \gamma = \frac{2}{3} \gamma^2 \phi^2 \quad (16)$$

where A is the matrix required to preserve the dyadic tensorial product in Voigt notation.

The equivalent plastic strain and band parameter increments are  ${}^{t+\Delta t} \bar{\varepsilon} = {}^t \bar{\varepsilon} + \bar{\varepsilon}$  and  ${}^{t+\Delta t} \gamma = {}^t \gamma + \gamma$ . We model the behavior of the band as rigid-plastic, thus being active only in loading. As we keep the shear band direction constant for every localized element eq. (9) has to be fulfilled along every incremental deformation step, therefore the stress tensor has to evolve radially,

$${}^{t+\Delta t} \sigma_{ij} = k \ {}^t \sigma_{ij} \ , \ k \geq 1 \quad (17)$$

During the deformation process, the material remains in the plastic range, hence its yield stress evolves radially,

$${}^{t+\Delta t} \sigma_y = k \ {}^t \sigma_y \quad (18)$$

As a consequence of these radial evolutions band forces evolve radially; hence,

$${}^{t+\Delta t} \underline{F}_{sb} = k \ {}^t \underline{F}_{sb} \quad (19)$$

and so with  ${}^t H$  the hardening at time t,

$${}^{t+\Delta t} \underline{F}_{sb} = {}^t \underline{F}_{sb} \left( 1 + \frac{\sqrt{2/3} \ {}^t H \phi \gamma}{{}^t \sigma_y} \right) \quad (20)$$

Replacing eqns. (13), (14) and (20) into eq. (12) and solving for  $\delta U$  and  $\delta \gamma$  we get,

$$\begin{bmatrix} {}^t \underline{K}_u & -{}^t \underline{K}_u \underline{\Theta} \\ -\underline{\Theta}^T {}^t \underline{K}_u & \underline{\Theta}^T {}^t \underline{K}_u \underline{\Theta} + \underline{\Theta}^T \underline{F}_{sb} \left( \frac{\sqrt{2/3} \ {}^t H \phi \gamma}{{}^t \sigma_y} \right) \end{bmatrix} \begin{bmatrix} \underline{U} \\ \gamma \end{bmatrix} = \begin{bmatrix} {}^{t+\Delta t} \underline{R} - {}^t \underline{F} \\ \underline{\Theta}^T ({}^{t+\Delta t} \underline{F}_{sb} - {}^t \underline{F}_{sb}) \end{bmatrix} \quad (21)$$

where,

$$\begin{aligned} {}^t\mathbf{K}_u &= \int_{V_1+V_2} \mathbf{B}^T {}^{t+\Delta t}\mathbf{C}^{Ep} \mathbf{B} \, dv \\ {}^{t+\Delta t}\mathbf{R} &= \int_{S_1+S_2} \mathbf{H}^T {}^{t+\Delta t}\mathbf{p} \, dv \quad (22) \\ {}^t\mathbf{F} &= \int_{S_1+S_2} \mathbf{B}^T {}^t\boldsymbol{\sigma} \, dv \end{aligned}$$

Since the above eq. (21) corresponds to the linearized step we have to iterate for solving the incremental step using Newton iterations (see for example [Bathe 1996](#)).

## 5 NUMERICAL RESULTS

To test the new formulation we present a plane strain unidirectional extension specimen using J2 plasticity for an elastic/ perfectly plastic material model, see figure 4. In the examples we consider a material with  $E=200\text{GPa}$ ,  $\nu = 0.3$ ,  $\sigma_y = 600\text{MPa}$ . The localization is induced by a reduction of 50% in the yield stress of the corner element.

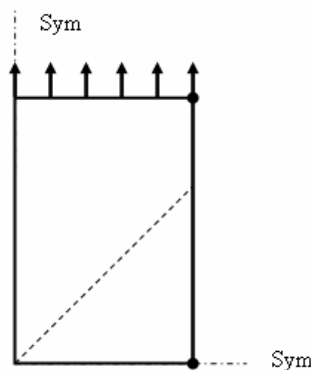


Figure 4: Plane strain test

In figure 5, 6 and 7 we present convergence studies for the elements Q1P0, Q2P1 and QMITC using undistorted elements which display an excellent convergence when the mesh is refined without showing mesh dependency. The plastic energy dissipated by the continuum, which as expected decreases for localized elements when the mesh is refined and the plastic energy dissipated by the localization modes, which as expected increases when the mesh is refined. In figure 8 results for the  $16 \times 24$  mesh are plotted for regular and distorted meshes for element QMITC.

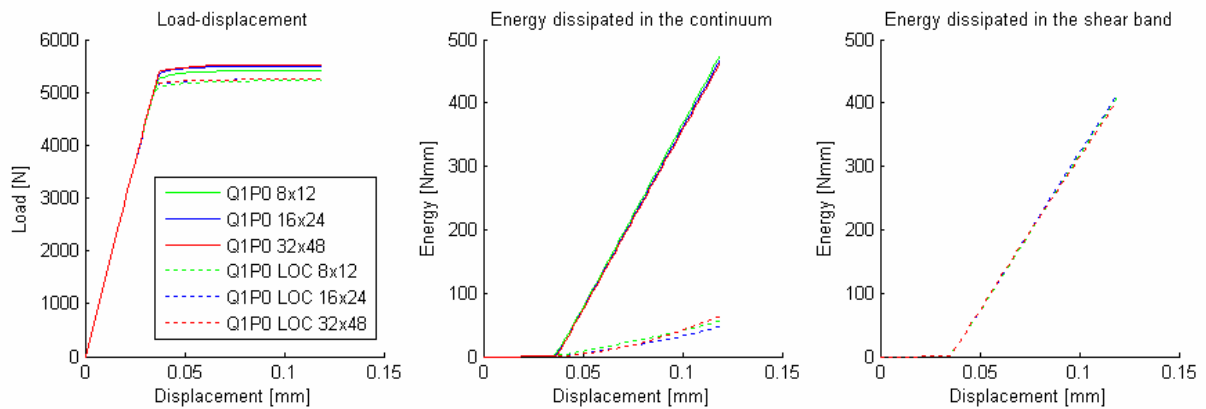


Figure 5: Element Q1P0 convergence studies

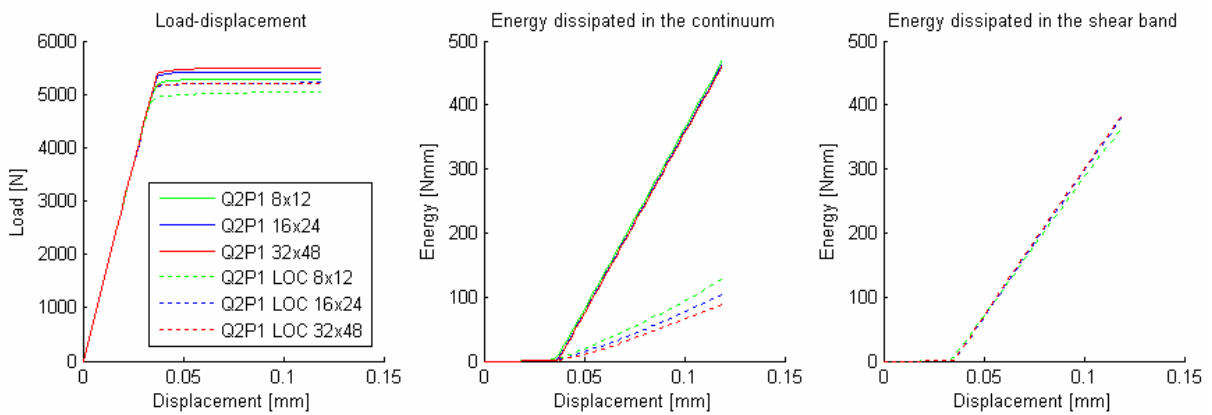


Figure 6: Element Q2P1 convergence studies

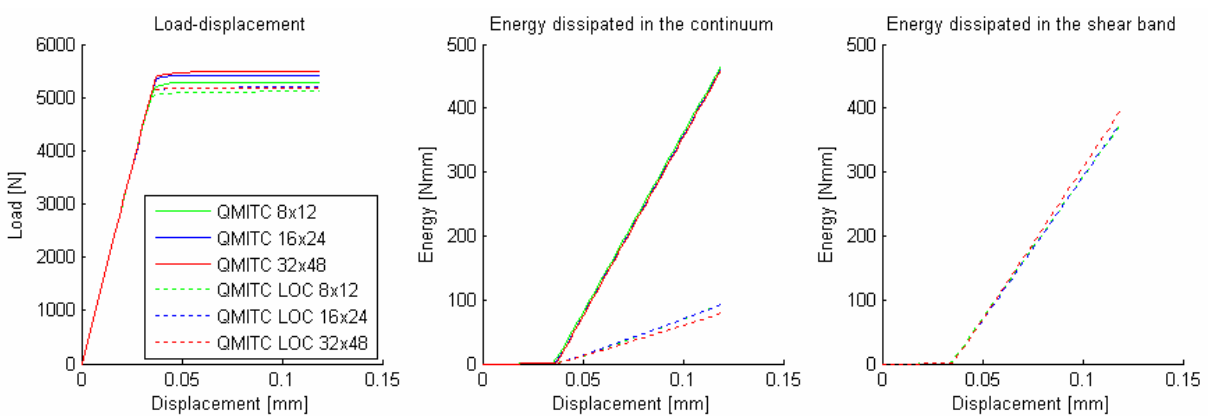


Figure 7: Element QMITC convergence studies

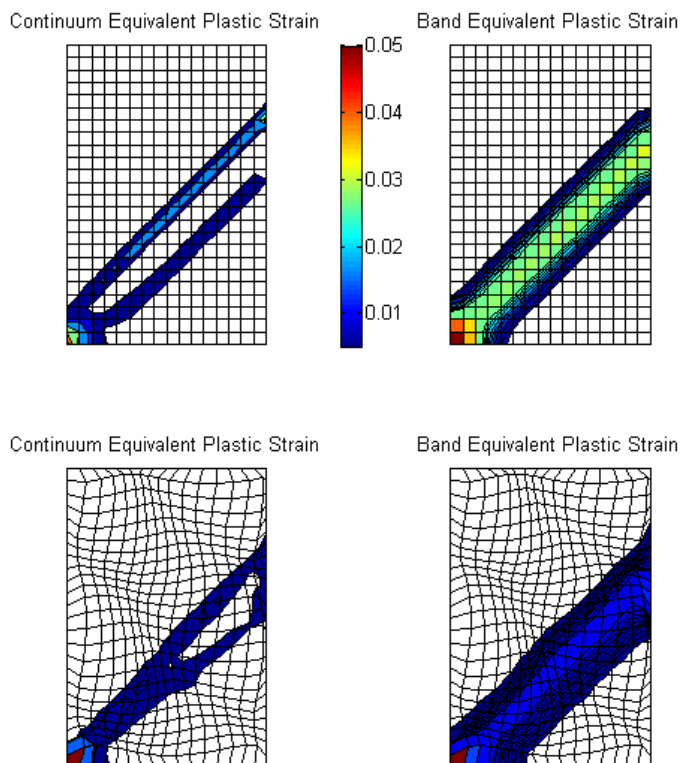


Figure 8: Equivalent plastic strain for element QMITC in distorted and undistorted meshes

For the sake of completeness, we present results in figure 9 for material with softening plastic behavior with  $ET = -E/10^2$  and  $E = 200\text{GPa}$ ,  $\nu = 0.3$  and  $\sigma_y = 600\text{MPa}$ . We present, the results obtained in simple traction using the standard QMITC element formulation and the element enhanced with localization modes. The standard formulation provides a very mesh dependent post-yielding result; however, the result produced by our new formulation is quite mesh independent.

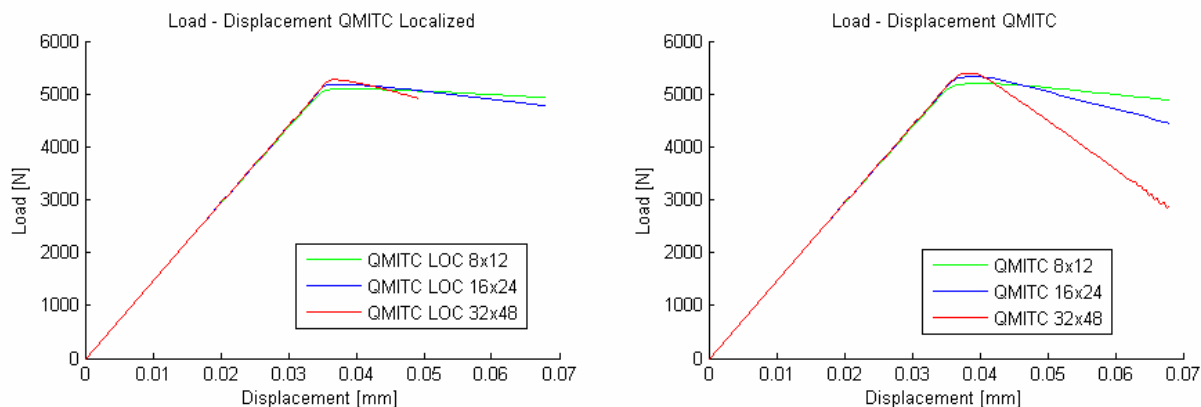


Figure 9: Localization response to material softening

## 6 CONCLUSIONS

A two-scale finite element formulation for modeling shear band localizations in J2 plastic deformation processes based on the use of embedded strong discontinuity modes triggered via a stress based criterion has been discussed. The formulation has been implemented in QMITC, Q1P0 and Q2P1 elements with similar results.

From the physical point of view, the new formulation does not require the definition of non-physical strain softening stress/strain relations and does not use material properties like fracture energy, which have not been defined nor measured in the environment of J2 plasticity.

Regarding mesh aspects, it does not require a specific mesh refinement to model the localization phenomena, provides mesh independent results even if a softening stress/strain relation is used and results are quite insensitive to element distortions.

Implementation is quite straight forward as the localization algorithm lives at element level, uses the same integration rules and schemes as the standard elements and localization parameters appear at element level and can be condensed out before assembly.

Acknowledgement: We gratefully acknowledge the support of TENARIS for this research.

**REFERENCES.**

- Bathe K. J., *Finite Element Procedures*, Prentice Hall, NJ, 1996.
- de Borst R. and Nauta P., "Non-orthogonal cracks in a smeared finite element model", *Engng. Computations*, 2, pp.35-46, 1985.
- D'hers S. and Dvorkin E. N., "Modelling shear bands in J2 plasticity using a two scale formulation via embedded strong discontinuity modes" (accepted for publication), 2008.
- Dvorkin E. N., Cuitiño A. M. and Gioia G., "Finite elements with displacement interpolated embedded localization lines insensitive to mesh size and distortions", *Int. J. Numerical Methods in Engng.*, 30, pp.541-564, 1990.
- Dvorkin E. N. and Assanelli A. P., "2D finite elements with displacement interpolated embedded localization lines: the analysis of fracture in frictional materials", *Comput. Meth. Appl. Mech. Engng.*, 90, pp.829-844, 1991.
- Dvorkin E. N., Assanelli A. P. and Toscano R. G., "Performance of the QMITC element in 2D elasto-plastic analyses", *Computers & Structures*, Vol.58, pp.1099-1129, 1996.
- Dvorkin E. N. and Goldschmit M. B., "Nonlinear Continua", Springer, Berlin, 2005.
- Hillerborg A., Modéer M. and Petersson P. E., "Analysis of crack formation and crack growth in concrete by means of fracture mechanics and finite elements", *Cement Concr. Res.*, 6, pp.773-782, 1976.
- Larsson R., Runesson K., Ottosen N. S., "Discontinuous displacement approximation for capturing plastic localization", *Int. J. Num. Methods in Engng.*, 36, 2087-2105, 1993.
- Mergheim J., Kuhl E. and Steinmann P., "A finite element method for the computational modelling of cohesive cracks", *Int. J. Numerical Methods in Engng.*, 63, pp.276-289, 2005.
- Moës N., Dolbow J. and Belytschko T., "A Finite Element Method for Crack Growth Without Remeshing," *Int. J. Numerical Methods in Engng.*, 46, pp. 131-150, 1999.
- Ortiz M., Leroy Y., Needleman A., "A Finite-Element Method for Localized Failure Analysis", *Comput. Meth. Appl. Mech. Engng.*, 61, pp.189-214, 1987.
- Ottosen N. S., Runesson K., "Properties of discontinuous bifurcation solutions in elasto-plasticity". *Int. J. Solids Structures*, 27, 401-421, 1991.
- Rice J. R., "The Localization of Plastic Deformation", in *Theoretical and Applied Mechanics (Proceedings of the 14th International Congress on Theoretical and Applied Mechanics, Delft, 1976, ed. W.T. Koiter)*, Vol. 1, North-Holland Publishing Co., pp.207-220, 1976.
- Simo J. C., and Hughes T.J.R., *Computational Inelasticity*, Springer, 1997.